ASTRONOMY & ASTROPHYSICS
SUPPLEMENT SERIES

Astron. Astrophys. Suppl. Ser. **98,** 127-135 (1993)

Observation of methanol maser sources with the Arcetri 12 GHz receiver

M.Catarzi, L.Moscadelli and D.Panella

Osservatorio Astrofisico di Arcetri, Largo E.Fermi 5, 50125, Florence, Italy

Received April 23; accepted July 20, 1992

Abstract. — We describe here the results of a test run made with a receiver built in Arcetri for the observation of the 12.178 GHz methanol maser line. We also report the description of a monitoring program of 12 GHz methanol masers which has been started with the 32 m Medicina antenna.

Key words: interstellar medium — maser — methanol

1. Introduction

Recently, many methanol transitions in the centimeter and millimeter regions have been detected as maser emission towards star forming regions. Unlike H_2O and OH masers, up to now no methanol maser emission has been observed towards circumstellar shells of late spectral type stars (Norris et al. 1987 ; Koo et al. 1988).

The marked separation between the detection probability of different transitions in different objects has led to the definition of two classes of methanol masers (Batrla et al. 1987 ; Menten 1991). The prototype of class I masers is Orion-KL, while W3(OH) is that of class II masers.

Class II methanol masers show several velocity components spread over a few km/s, while class I masers have few components confined to a velocity interval of less than 1 km/s. Sometimes class I spectra show narrow components of 0.3-0.7 km/s superimposed to a broad (quasi-) thermal emission.

The most important difference between the two classes of masers regards their place of formation. While class II methanol masers are observed near compact HII regions, IR sources and H_2O and OH masers, class I masers are found at distances of about 1 pc from these objects. Observational data (Plambeck et al. 1990) suggest that class I masers originate in shock fronts associated to powerful molecular outflows: class I masers can therefore be used to investigate the low mass star formation, where molecular ouflows are supposed to play a dominant role. On the contrary class II masers, being probes of the physical and kinematic conditions of the hot and dense molecular cores around compact HII regions, are very useful to study the formation and the first evolution of massive stars.

The most likely excitation mechanisms are thought to be for class I masers the collisional one, for class II masers the radiative pumping ; however, up to now, no model has been able to explain the population inversion of all the methanol transitions effectively detected as maser in a distinct region.

Among the class II masers very strong emission is observed at the 12.178 GHz frequency: towards W3(OH), NGC7538, NGC6334 its flux density is of the order of 1000 Jy (Batrla et al. 1987).

In the Arcetri observatory an uncooled low-noise receiver for the methanol line at 12 GHz has been built and tested in order to be used for *VLBI* observations (Wilson 1987, private communication) and for single dish spectroscopy.

2. Observations

The single dish spectral observations were carried out in June, November 1990 and January 1991 with the 32 m Medicina radiotelescope operated by the Istituto di Radioastronomia CNR. At 12.2 GHz the H.P.B.W. is 2'.5. The receiver front-end consists of a low-noise HEMT first stage followed by two stages of conventional FET amplification. The total system temperature was ≈180 K (SSB) (Catarzi et al. 1990).

The flux density calibration was obtained by continuum observations of DR21 (20.4 Jy) and 3C286 (4.01 Jy) (Baars et al. 1977). The resulting mean antenna efficiency was 0.12 K/Jy. The total uncertainty in the flux density scale is estimated about 20 %.

The spectra were obtained using the Arcetri digital 1024 channels autocorrelator in the total power mode

switching between the ON and OFF position. The used bandwidths lie in the range 0.78 MHz to 6.25 MHz, corresponding to a velocity resolution from 0.018 km/s to 0.15 km/s. The integration time was 5 minutes in the ON and OFF positions, resulting in a r.m.s. noise level on the "ON-OFF" spectra from about 1.5 Jy to about 5.5 Jy depending on the used bandwidth.

Both the autocorrelation function and the computed spectra are stored on files in a format conforming to the TOOLBOX package specifications. TOOLBOX is the line reduction package developed at the Max-Planck-Institut für Radioastronomie, Bonn (Cesaroni et al. 1988) and kindly made available to our group.

3. Results

In order to effect a first astronomical test of the receiver, we have prepared a list of all the methanol sources up to now detected at 12 GHz. (Norris et al. 1987 ; Batrla et al. 1987 ; Koo et al. 1988 ; Kemball et al. 1988).

The observed list includes all the methanol 12 GHz sources reported in the literature up to June 1990 which can be observed by the Medicina radiotelescope ($\delta > -30^o$), with the exception of TMC-1, L183, L183(CS) (these last three sources have been detected in absorption towards the 2.7 K cosmic background by Walsmley et al. (1988)).

3.1. *Comparison with the literature data*

We have compared our spectra of the detected sources with those extracted from literature.

We have detected emission only from 14 of the 27 sources included in our list. These detections are reported in Table 1: the coordinates and the radial velocity of the spectral characteristics are extracted from the literature, the bandwidth reported was choosen to obtain the maximum velocity resolution.

Likely, 10 non detections are due to the insufficient sensitivity of our system (for instance Batrla observes an absorption of about 0.2 Jy in S140,while our r.m.s. noise level is 1.9 Jy); the remaining 3 non detections (Sgr B2, Sgr B2S, W33-met) are due to strong interferences.

The spectra of the detected sources together with those extracted from the literature (when available, on the rigth) are reported in Fig.1. It is possible to note a strong resemblance of spectral profile.

Up to now, all the observations are pointing out the constancy in intensity and shape of the spectral profiles of class I and II methanol masers. Menten et al.(1988a) have shown that the variation in intensity (but not in shape) of the spectra of the 25 GHz J=6 and J=7 lines towards Orion-KL observed by Barrett et al.(1975) is interpretable as due to calibration errors rather than to a synchronous variation of all the maser components. The observations of Haschick et al.(1990) and Bachiller et al.(1990) of a number of 44 GHz masers indicate that no significant intensity variation has been taking place within a several month period. The comparison of our spectra with the literature ones points out that also the 12 GHz methanol masers are time stable on periods of 2 - 4 years. We think that the sometimes present difference in the intensity scale between our and literature measurements is due only to calibration error.

In Table 2 we report the Gaussian fit results: for each spectral component we give the intensity , the velocity and the F.W.H.M.

The peak velocity of our spectra is compared with that from the literature in Fig. 2: a good agreement can be noted.

3.2. *Selfconsistency*

The selfconsistency of our measurements has been verified by observing the same sources in different periods and comparing the results, relying on the stability of methanol masers.

In the three runs we obtained about 150 spectra.

The main results of our observations are:

1. All the sources with structured spectra (among which W3(OH), NGC7538, G188.94+0.89, Cepheus A, G9.62+0.89) show a highly stable profile. In all cases, the relative intensities of the spectral components are constant within the Gaussian fit errors and the indetermination due to the receiver noise; typically we observe a variation lower than 5% .
2. The absolute flux density variation is less than our calibration error of 20% for flux densities between 10 and 1000 Jy.

For 8 sources a comparison between the mean peak flux densities of two different runs are reported in Fig.3. Error bars express our 20% error estimation.

3.3. *Non detected sources*

The upper limits of our non detections are reported in Table 3. For each source name, coordinates one or more velocity ranges and the 3σ noise level are given. "Int. " in the last column means interferences in the spectra.

3.4. *Interferences*

The methanol maser line at 12.2 GHz lies in the satellite broadcasting bandwidth; this means that there is a high probability to have strong interferences in the spectra . At the present time we have no particular correlation between the antenna position (Az, El) and the interferences, except in the case of well known positions of the satellites in the sky. In any case, after each observation which may

show the presence of a new line, it is necessary to look at the source with other antenna positions in order to avoid false detections.

4. Conclusions

We have designed and built a 12.2 GHz receiver to observe the $2_0 - 3_{-1}$ E methanol transition. Laboratory tests and first spectral observations show that its stability and sensitivity are satisfactory for our purposes.

Our observations point out the time stability of methanol maser sources on a time scale of the order of 2-8 months. The comparison of our observations with the literature let us extend the time stability scale to periods of 2-4 years depending on the examined source.

Acknowledgements. The authors are grateful to Prof. M. Felli for suggesting and revising this work and to the technical staff of Arcetri and Bologna CNR for the help and assistance during the observations.

References

Baars J.W.M., Genzel R., Pauliny-Toth I.I.K., Witzel A. 1977, A&A, 61, 99
Bachiller R., Menten K.M., Gomez-Gonzales J., Barcia A. 1990, A&A, 240, 116
Barrett A.H., Schwartz P.R., Waters J.W. 1971, ApJ, 168, L101
Barrett A.H., Ho P., Martin R.N. 1975, ApJ, 198, L119
Batrla W., Matthews H.E., Menten K.M., Walmsley C.M. 1987, Nat, 326, 49
Catarzi M., Curioni P., Curioni G.P., Moscadelli L., Panella D., Tofani G. Arcetri Tech. Rep. 1/1990
Cesaroni R., Comoretto G., Massi M., Palagi F. Arcetri Tech. Rep. 5/1988
Haschick A.D., Menten K.M., Baan W.A. 1990, ApJ, 354, 556
Kemball A.J., Gaylard M.J., Nicolson G.D. 1988, ApJ, 331, L37
Koo B.C., Williams D.R.W., Heiles C., Backer D.C. 1988, ApJ, 326, 931
Menten K.M., Walmsley C.M., Henkel C., Wilson T.L. 1988, A&A, 198, 267 (a)
Menten K.M., Reid M.J., Moran J.M., Wilson T.L., Johnston K.J., Batrla W. 1988, ApJ, 333, L83 (b)
Menten K.M. 1991, Proceedings of the Third Haystack Observatory Meeting, ed. A.D. Haschick & P.T.P. Ho, p.119, San Francisco: Astronomical Society of the Pacific.
Morimoto M., Ohishi M., Kanzawa T. 1985, ApJ, 288, L11
Norris R.P., Caswell J.L., Garder F.F., Wellington K.J. 1987, ApJ, 321, L159
Norris R.P., McCutcheon W.H., Caswell J.L., Wellington K.J., Reynolds J.E., Peng R.S., Kesteven M.J. 1988, Nat, 335, 149
Plambeck R.L., Menten K.M. 1990, ApJ, 364, 555
Walmsley C.M., Batrla W., Matthews H.E., Menten K.M. 1988, A&A, 197, 271
Wilson T.L., Walmsley C.M., Snyder L.E., Jewell P.R. 1984, A&A, 134, L7
Wilson T.L., Walmsley C.M., Menten K.M., Hermsen W. 1985, A&A, 147, L19

Table 1. Detected sources

Name	α	δ	Rad.vel (km/s)	Band (MHz)	Bib. ref.
W3(OH)	02 23 16.4	61 38 57.7	-46.0 , -42.0	0.78	4
G188.94+0.89	06 05 53.7	21 39 09.0	10.0 , 12.0	0.78	1
G9.62+0.19	18 03 16.0	-20 32 01.0	-5.0 , 5.0	1.56	1
IRAS 18056-1952	18 05 38.7	-19 52 34.0	74.2, 75.6	1.56	5
IRAS 18089-1732	18 08 56.4	-17 32 14.0	38.5, 40.0	1.56	5
G12.68-0.18	18 10 58.9	-18 02 39.0	56.8	1.56	1
G12.91-0.26	18 11 44.2	-17 52 58.0	40.0	25.0	2
G15.04-0.68	18 17 31.6	-16 12 58.0	22.0	0.78	2
W43S	18 43 26.7	-02 42 40.0	96.5	1.56	1
G31.29+0.07	18 45 36.8	-01 29 12.0	109 ,113	6.25	1
W48	18 58 12.8	01 09 13.0	40.0 , 46.0	0.78	1
W51	19 21 23.8	14 24 52.0	60.0	1.56	3
Cepheus A	22 54 27.0	61 45 46.0	-4.3	0.78	1
NGC7538	23 11 36.5	61 11 47.0	-62.0 , -56.0	1.56	1

1. Koo (1988)
2. Norris (1987)
3. Batrla (1987)
4. Menten (1988b)
5. Kemball (1988)

Table 2. Gaussian fit results

Name	peak (Jy)	±	vel. (km/s)	±	F.W.H.M. (km/s)	±
W3(OH)	476.0	7.7	-45.30	0.28E-2	0.339	0.67E-2
	862.9	5.0	-44.62	0.26E-2	0.746	0.11E-1
	494.8	10.1	-44.02	0.23E-2	0.268	0.65E-2
	550.7	4.1	-43.36	0.43E-2	0.896	0.12E-1
	81.4	7.2	-42.41	0.11E-1	0.239	0.26E-1
G188.94+0.89	221.3	2.2	10.53	0.49E-2	0.409	0.88E-2
	133.7	3.7	10.96	0.85E-2	0.345	0.29E-1
	156.7	6.2	11.29	0.79E-2	0.292	0.11E-1
G9.62+0.19	17.0	1.2	-0.47	0.30E-1	0.841	0.72E-1
	117.0	3.7	1.17	0.21E-2	0.164	0.64E-2
	55.1	1.9	1.41	0.14E-1	0.599	0.22E-1
	14.7	3.0	2.94	0.17E-1	0.188	0.47E-1
	18.2	1.3	3.50	0.36E-1	0.807	0.92E-1
IRAS 18056-1952	20.3	1.5	74.88	0.17E-1	0.460	0.40E-1
IRAS 18089-1732	70.4	1.9	39.17	0.43E-2	0.333	0.10E-1
G12.68-0.18	10.4	1.3	56.89	0.35E-1	0.560	0.87E-1
	9.2	1.5	57.77	0.35E-1	0.419	0.84E-1
G12.91-0.26	17.8	1.6	46.28	0.52E-1	0.940	0.90E-1
G15.04-0.68	13.8	2.4	21.30	0.18E-1	0.219	0.43E-1
	13.8	2.2	23.30	0.19E-1	0.248	0.46E-1
W43S	32.5	2.5	96.10	0.48E-1	0.570	0.79E-1
	52.6	3.2	96.69	0.27E-1	0.522	0.43E-1
G31.29+0.07	79.9	2.1	110.28	0.57E-2	0.460	0.15E-1
	10.2	1.1	111.69	1.20E-1	1.690	3.30E-1
	14.2	2.6	112.59	0.27E-1	0.350	0.82E-1
W48	30.1	1.4	40.75	0.32E-1	0.759	0.75E-1
	107.1	3.1	41.31	0.40E-2	0.324	0.11E-1
	30.2	1.7	41.92	0.15E-1	0.512	0.42E-1
	24.9	2.1	44.03	0.11E-1	0.271	0.28E-1
	97.0	7.9	44.48	0.45E-2	0.232	0.13E-1
	43.6	2.3	44.77	0.35E-1	0.459	0.59E-1
	8.5	1.5	46.12	0.45E-1	0.55	0.11
W51	13.5	3.1	55.75	0.16E-1	0.126	0.38E-1
	15.2	2.2	56.01	0.21E-1	0.262	0.56E-1
CepheusA	128.8	2.2	-4.15	0.16E-2	0.187	0.38E-2
	6.8	2.6	-1.78	0.26E-1	0.143	0.63E-1
NGC7538	37.4	2.5	-61.32	0.13E-1	0.290	0.28E-1
	20.8	1.9	-60.86	0.31E-1	0.466	0.75E-1
	225.7	1.4	-56.33	0.23E-2	0.779	0.56E-2

Table 3. Upper limits list

Name	α	δ	Vel.Range(km/s)	3σ Limit(Jy)
W3	02 21 56.6	61 52 30.0	-115, 40	5.4
Orion - KL	05 32 46.7	-05 24 21.0	-25, 48	8.4
NGC 2024	05 39 11.4	-01 56 09.0	-20, 50	7.5
S255	06 09 58.1	18 00 16.0	25, 60	7.2
" " "	" " "	" " "	-20, 80	7.5
S269	06 11 46.5	13 50 39.0	4, 37	12.0
IRC +10216	09 45 14.8	13 30 39.0	-60, 10	7.8
Sgr A	17 42 27.8	-29 03 59.0	-18, 58	6.0
Sgr B2	17 44 10.5	-28 21 58.0	45, 80	Int.
Sgr B2(S)	17 44 10.5	-28 23 14.0	50, 56	12.0
" " "	" " "	" " "	56, 60	Int.
" " "	" " "	" " "	60, 70	12.0
G0.55-0.85	17 47 03.9	-28 53 42.0	-20, 60	8.4
G8.67-0.36	18 03 18.6	-21 37 59.0	34, 53	Int.
W31	18 07 30.5	-19 56 29.0	-15, 20	9.0
W33	18 11 17.9	-17 56 45.0	0, 40	7.2
" " "	" " "	" " "	40, 73	Int.
RCW 169	18 28 16.1	-09 51 01.0	15, 55	8.1
W49 N	19 07 49.5	09 01 15.0	-2.5,32.5	11.1
K3 - 50	19 59 50.0	33 24 18.0	-35, 0	10.5
DR21	20 37 13.9	42 08 54.0	-75, 75	5.4
" " "	" " "	" " "	-10, 6	10.8
DR21 (OH)	20 37 14.8	42 12 08.0	-75, 75	5.8
S140	22 17 41.1	63 03 40.0	-60, 65	5.4

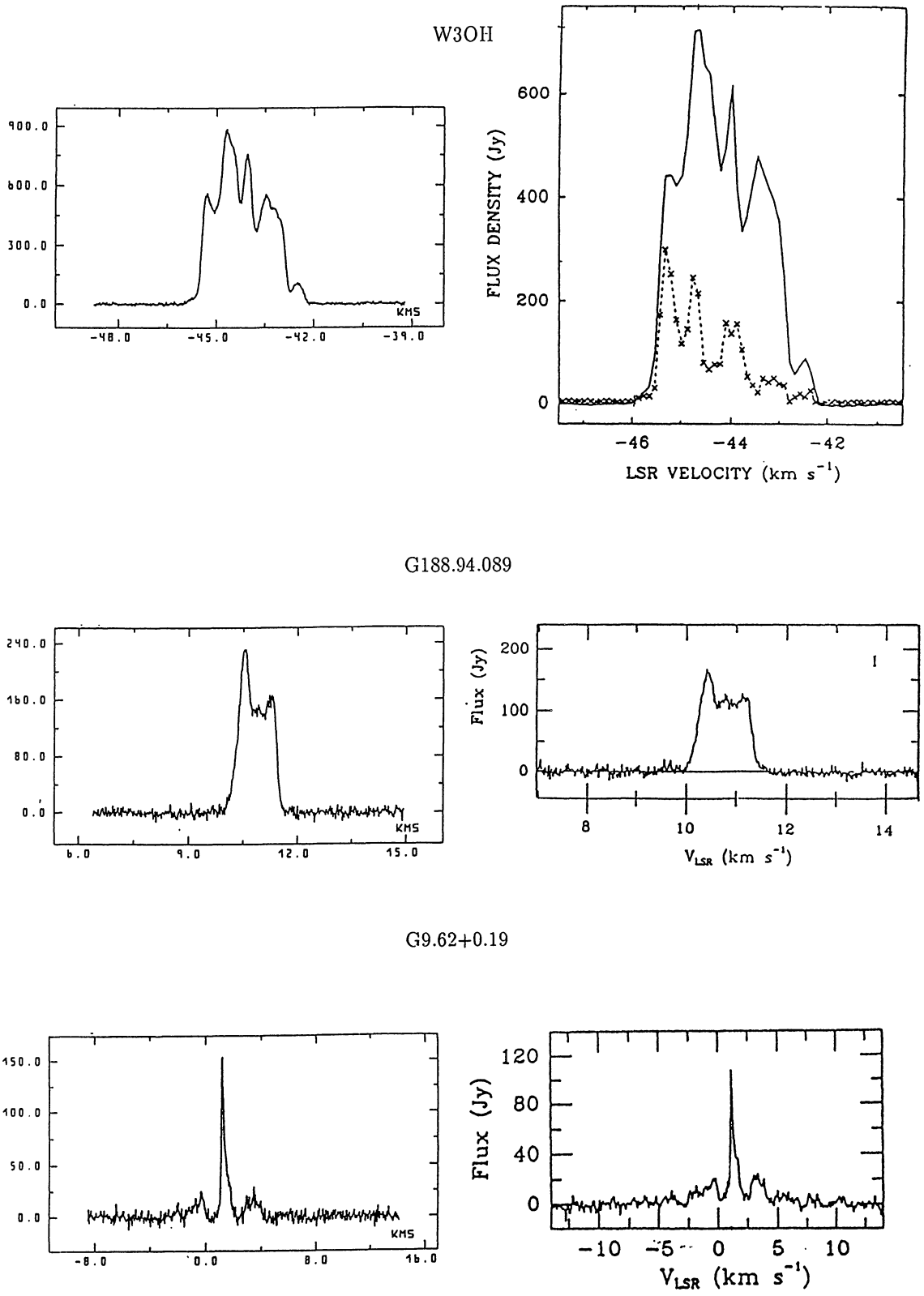

Fig. 1. Detected sources spectra

IRAS 18056-1952

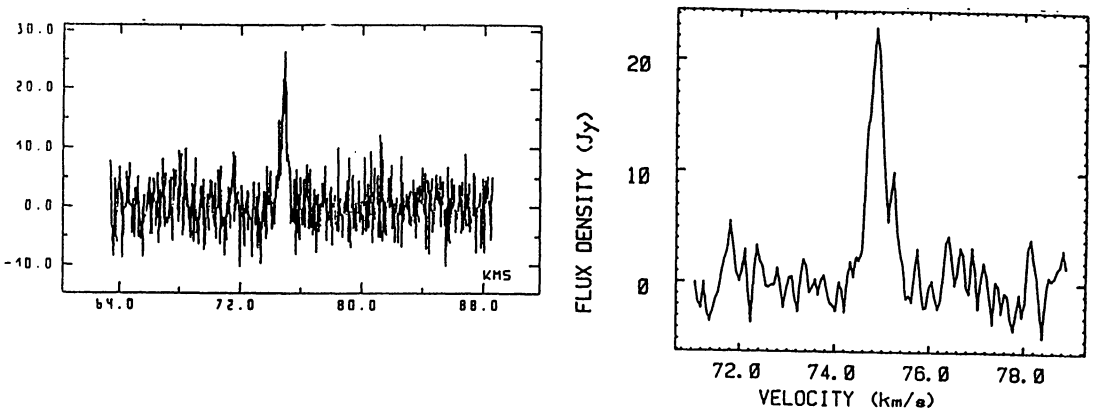

IRAS 18089-1732

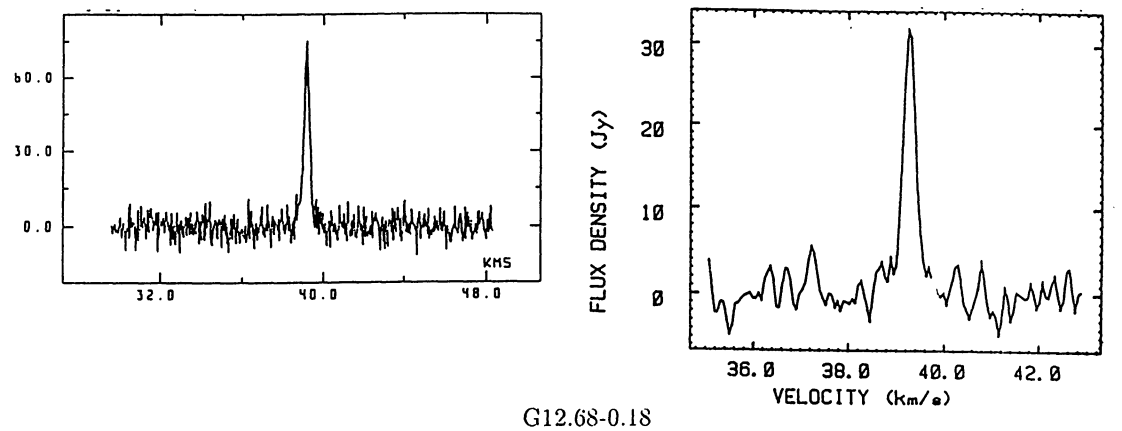

G12.68-0.18

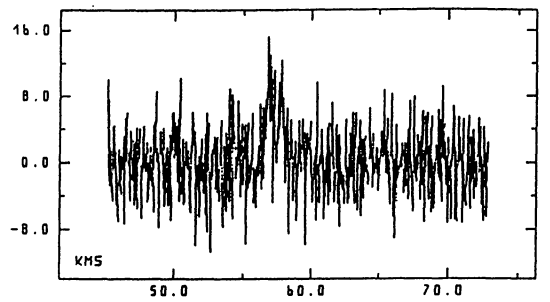

Fig. 1. continued

G12.91-0.26

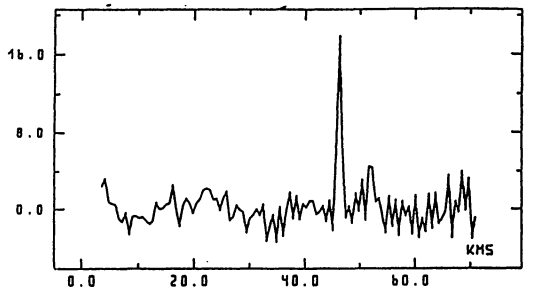

G15.04-0.68

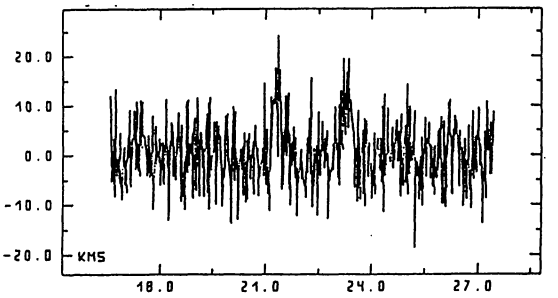

W43S

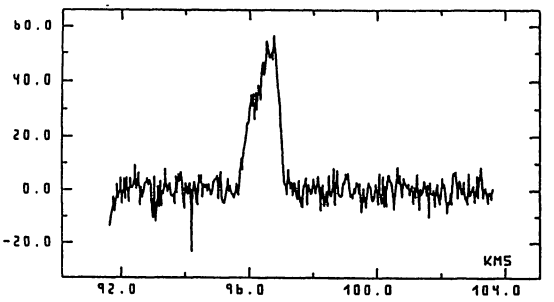

Fig. 1. continued

G31.29+0.07

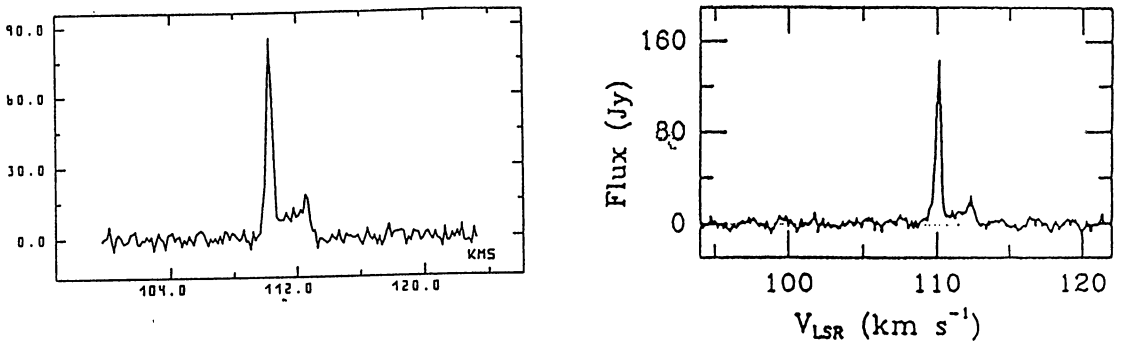

W48

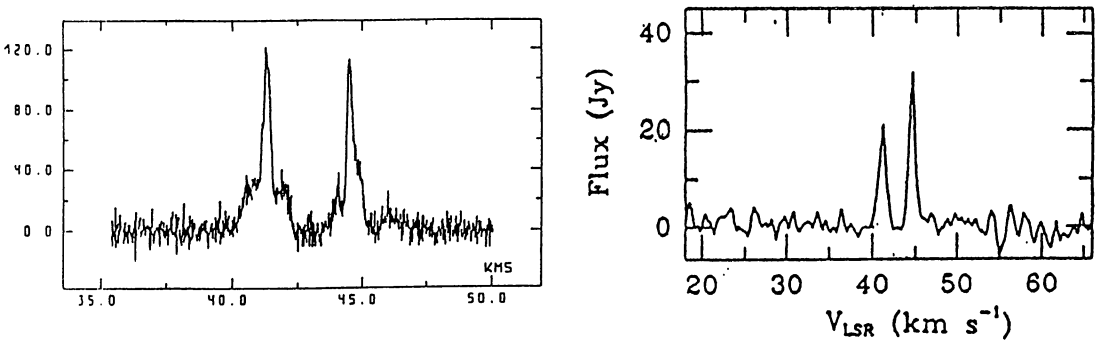

W51

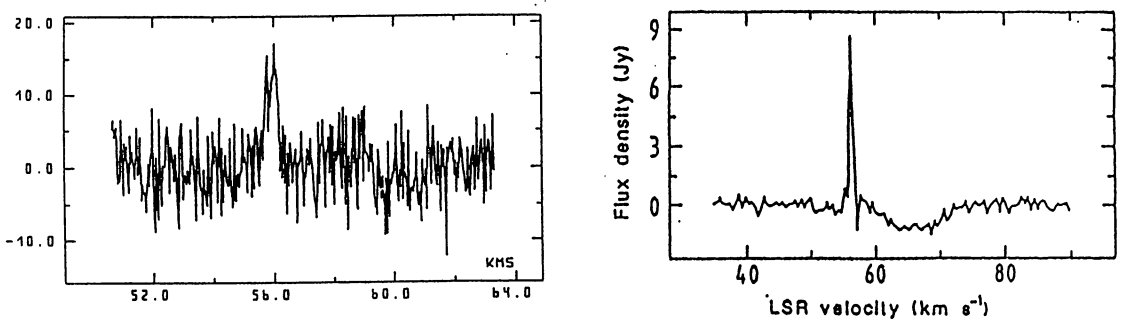

Fig. 1. continued

Cepheus A

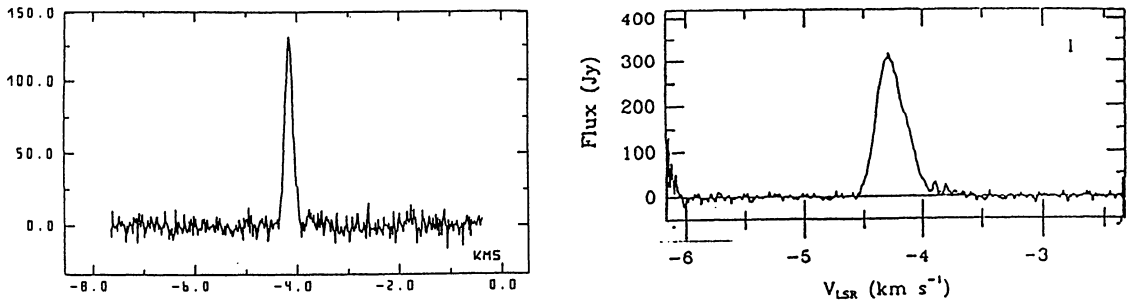

NGC7538

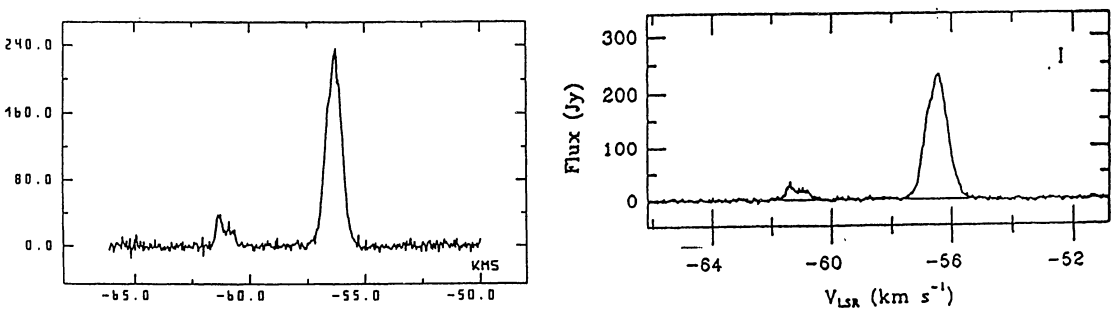

Fig. 1. continued

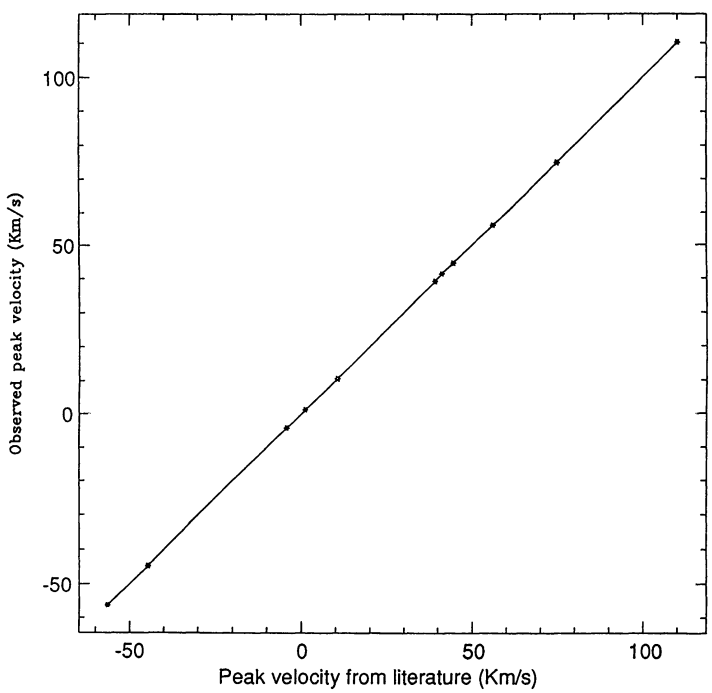

Fig. 2. Peak velocity comparison

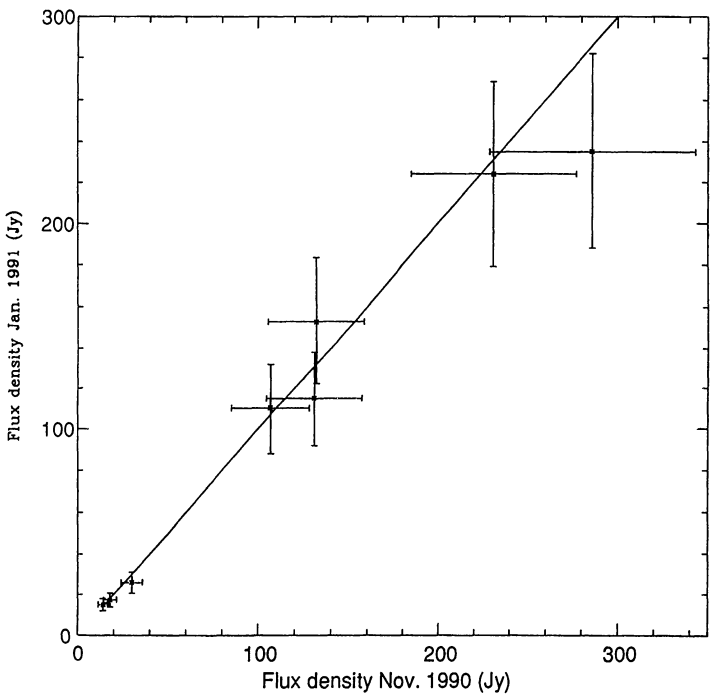

Fig. 3. Peak flux comparison